

# Variable-Temperature Solid-State $^{13}\text{C}$ NMR Studies of Nascent and Melt-Crystallized Polyethylene

Frederick G. Morin,<sup>\*,†</sup> G. Delmas,<sup>‡</sup> and D. F. R. Gilson<sup>†</sup>

Department of Chemistry, McGill University, 801 Sherbrooke West, Montreal, PQ, H3A 2K6 Canada, and Département de Chimie, Université du Québec à Montreal, C.P. 8888 Succ. A, Montreal, PQ, H3C 3P8 Canada

Received May 2, 1994; Revised Manuscript Received February 17, 1995<sup>\*</sup>

**ABSTRACT:** Nascent and melt-crystallized ultrahigh molecular weight polyethylene (PE) have been studied using solid-state  $^{13}\text{C}$  NMR spectroscopy. Significant differences between the two materials are observed in the CPMAS spectra particularly at elevated temperatures. Three separate resonances are observed in nascent samples when the temperature is raised to near the melting point, the third peak being of an intermediate chemical shift between the crystalline and amorphous resonances that are observed in the spectra of melt-crystallized samples. Based on this chemical shift, the third resonance is likely due to polymer chains which undergo conformational averaging which is intermediate between the rigid all-trans crystalline polymer and very mobile amorphous chains. Evidence is reported which shows that this is material that is present in nascent PE below the melting point and is not created during the melting process. These observations are confirmed by the measurement of 2D wide-line separation (WISE) experiments where the  $^1\text{H}$  line width of the amorphous component of melt-crystallized PE is much narrower than that of a nascent sample. Numerous nascent PE samples, including those of low molecular weight, display similar spectral features.

## Introduction

Polyethylene (PE) has been the subject of numerous NMR investigations. Extensive  $^2\text{H}$  NMR studies of the motional properties of PE chains in the amorphous phase have been performed by Spiess and co-workers.<sup>1-5</sup> They employed solid-echo and spin alignment techniques to generate spectra whose line shapes could be analyzed in terms of highly constrained chain motion involving 3, 5, or  $\geq 7$  bonds depending on temperature.<sup>2,3</sup>  $^{13}\text{C}$  NMR has been used to investigate the overall phase structure of PE<sup>6-8</sup> as well as both spin<sup>9</sup> and chain diffusion.<sup>10</sup> A simple  $^{13}\text{C}$  CPMAS (cross polarization/magic angle spinning)<sup>11</sup> spectrum typically<sup>6-8,12</sup> consists of a peak at 33.1 ppm due to the all-trans polymer chains within the orthorhombic crystal structure, plus a broader peak at about 31 ppm due to the noncrystalline domains wherein the polymer chains undergo significant motion and the  $\gamma$ -gauche interaction present in the gauche conformation causes an upfield shift.<sup>13</sup> Spin diffusion between the phases has been measured in oriented samples,<sup>9</sup> while two-dimensional  $^{13}\text{C}$  MAS exchange spectroscopy<sup>10</sup> has demonstrated that chain diffusion occurs between the amorphous and crystalline phases at elevated temperatures.

However, these solid-state NMR studies of polyethylene have centered for the most part on melt-crystallized samples. Nascent PE, i.e., PE isolated from the reaction vessel without subsequent melt processing, has been less extensively studied, although Jarrett et al.<sup>14</sup> recently demonstrated that  $^{13}\text{C}$  CPMAS can be used to study the crystalline morphology of such materials as a function of both the synthesis conditions and annealing temperatures. Samples produced when the reaction was carried out at room temperature showed a strong peak at 34.2 ppm from the monoclinic crystalline form which disappeared when the samples were heated above 60 °C.<sup>14</sup>

Our motivation to study nascent PE stems from previous microscopy and fast differential scanning calorimetry (DSC) studies of nascent PE which revealed that polymerization produces a unique morphology.<sup>15,16</sup> The DSC study<sup>16</sup> showed nascent samples have a melting point that is 5–10 °C higher than samples which are melt-crystallized, an observation that was attributed to the presence of a morphology possessing considerable strain. The rapid release of heat during polymerization initially creates a molten globule of polymer on the surface of the catalyst which expands as new monomer units are added. Since there are numerous closely spaced polymerization sites on the catalyst, there is ready opportunity for polymer chains from different globules to entangle as the molten globules meet one another and before crystallization begins. Subsequent cocrystallization occurs after the outer layers are sufficiently far removed from the catalytic site. This outer crystallized material is constantly displaced and deformed by the expanding center of the globule, and therefore crystallization occurs in a shear field in the melt resulting in an overall strained structure.<sup>15,16</sup> It was noted very early that the crystals grown under shearing conditions have a different morphology than those grown in a quiescent solution.<sup>16,17</sup> Thus, nascent samples of PE have a morphology and melting behavior similar to that of PE crystallized under shear.

The concept of strain in semicrystalline polymers is not unique to nascent material. In general, there are a number of other ways to introduce strain into polymers: (a) it may be introduced in a film by stretching it (the melting temperature ( $T_m$ ) of an elongated film again being higher than  $T_m$  in the absence of stretching if tension is maintained during melting), (b) it can be introduced into the chains of chemical networks by swelling with a solvent (if parts of the swollen network are crystalline, then they will also melt at a higher temperature, although in this case it is not necessary to apply external tension since the presence of the solvent and the chemical cross-links in the chains is sufficient to hold the tension),<sup>18</sup> and (c) if the cross-links

<sup>†</sup> McGill University.

<sup>‡</sup> Université du Québec à Montreal.

<sup>\*</sup> Abstract published in *Advance ACS Abstracts*, April 1, 1995.

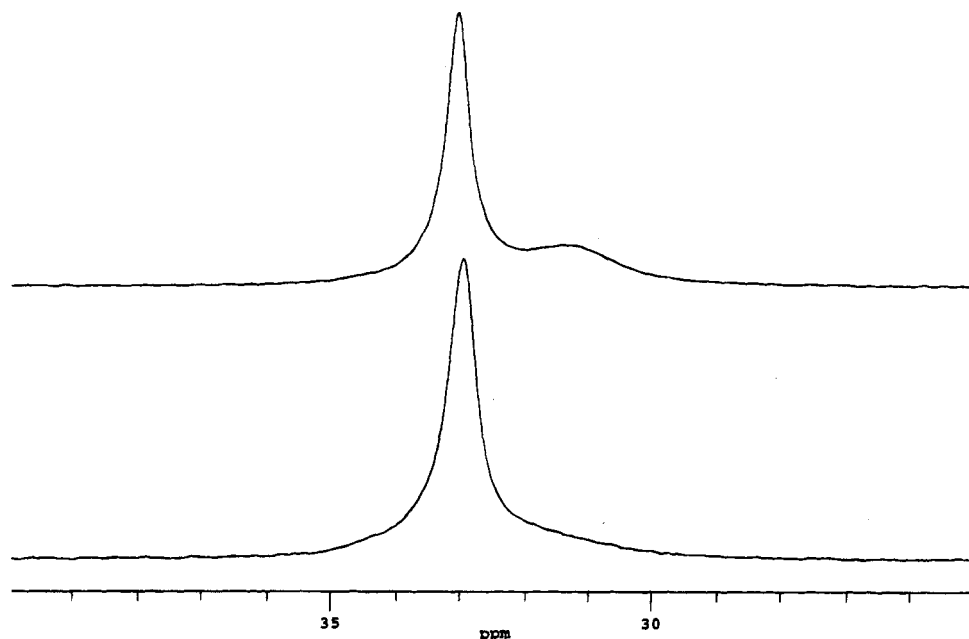


**Figure 1.**  $^{13}\text{C}$  CPMAS spectra of nascent PE (bottom) and melt-crystallized PE (top) at room temperature. Contact time was 1 ms.

are physical, due to chain entanglements instead of chemical cross-links, some strain exists at any temperature. This latter situation is most relevant here. However, during melting of a physical network complex phenomena occur which actually increase strain. One of them is the inescapable increase of volume (20%) during melting.<sup>19</sup> Because of the entangled chains, the temperature of the maximum of the melting peak in the DSC is delayed toward higher temperature as a result of the process of expansion. Thus the phase change between the crystalline state and the melt has an effect similar to that of the swelling action of solvent. (The melting traces and the range of persistence of birefringence of the melt of physical networks have been extensively studied by several groups.<sup>20</sup> The term used there is extended and oriented tie molecules rather than physical networks.) Also, WAXR evidence for the presence of a semiordered phase in the melt has been reported for nascent polymer and for chemically cross-linked samples of PE.<sup>17</sup>

The aim of this paper is to obtain information on the differences between nascent and melt-crystallized PE, on the transformation which takes place during the first melting and to see if it is possible to identify morphological features unique to nascent PE.

## Experimental Section

NMR spectra were obtained on an as-received sample of linear PE (Hostelen GUR 413 from Hoescht) whose nominal molecular weight was  $0.9 \times 10^6$ . Its density ( $0.94 \text{ g cm}^{-3}$ ), its heat of fusion ( $190 \text{ J g}^{-1}$ ), and its X-ray diffraction pattern indicate a crystalline fraction of 0.66. The temperature of fusion,  $T_m$  (i.e., the maximum in the melting endotherm), is  $140^\circ\text{C}$ . The degree of crystallinity is unchanged by melting and recrystallizing, but  $T_m$  is lowered to  $134^\circ\text{C}$ .

Variable-temperature CPMAS spectra were obtained on a Chemagnetics CMX-300 spectrometer operating at 75.3 MHz using a Chemagnetics PENCIL probe with 7.5 mm zirconia rotors. Spinning speeds were about 3 kHz, sufficient to eliminate spinning side bands. The decoupler frequency (about 1.5 ppm from TMS in the  $^1\text{H}$  frequency domain) and amplitude (60 kHz) were adjusted to give the narrowest possible line width for the orthorhombic peak at room temperature. Chemical shifts in the CPMAS spectra were obtained by fitting to

Lorentzian functions using the PEAKFIT program (Jandel Scientific Co.) and are reported relative to TMS by assigning a shift of 33.1 ppm to the orthorhombic peak in the room temperature spectrum. This resonance was found to be independent of temperature.

The variable-temperature experiments on nascent samples were performed by raising the temperature in increments, typically  $20^\circ\text{C}$ , and maintaining the sample at the new temperature for  $1/2$ –1 h while spectra were obtained. This was done up to and past the melting point of the orthorhombic crystals of the sample ( $140^\circ\text{C}$ ). These spectra were obtained with a contact time of 200  $\mu\text{s}$ .

## Results

**CPMAS Spectra.** Room-temperature  $^{13}\text{C}$  CPMAS spectra of nascent (bottom) and melt-crystallized PE (top) are given in Figure 1. The spectrum of nascent PE is typical of samples synthesized at a sufficiently high temperature to create only a minor amount of the monoclinic crystalline form.<sup>14</sup> It is dominated by the usual orthorhombic peak plus a broad high-field shoulder from the noncrystalline component. The spectrum of melt-crystallized PE (Figure 1, top) taken under the same conditions shows a distinctly separate resonance for the amorphous fraction at 31.5 ppm. The resonance from the crystalline peak of the nascent PE is broader than the corresponding resonance in the melt-crystallized sample, reflecting the less perfect nature of the phase in unprocessed samples.<sup>15,16</sup>

To best illustrate the differences observed between melt-crystallized and nascent PE, their  $^{13}\text{C}$  CPMAS spectra taken at  $101^\circ\text{C}$  are shown in parts A and B of Figure 2, respectively. The amorphous resonance in the nascent sample is downfield of the corresponding resonance from the melt-crystallized sample, indicative of more trans and less gauche contribution to the conformational averaging. The crystalline orthorhombic peak remains relatively unchanged as the nascent sample is heated until  $70$ – $90^\circ\text{C}$  when it broadens noticeably; the amorphous resonance sharpens and moves slowly to higher field as molecular mobility increases and the gauche effect on the chemical shift increases.<sup>13</sup> The spectra at  $128$  and  $137^\circ\text{C}$  are particularly interesting.

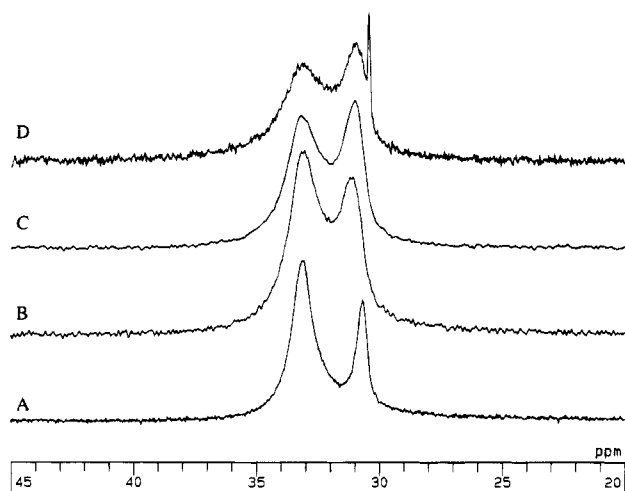


**Figure 2.**  $^{13}\text{C}$  CPMAS spectra of PE. All were obtained with a  $200\ \mu\text{s}$  contact time. (A) Spectrum of a melt-crystallized PE sample at  $101\ ^\circ\text{C}$ . The crystalline resonance appears at  $33.1\ \text{ppm}$ , and the resonance from the very mobile amorphous chains is at  $30.7\ \text{ppm}$ . (B) Spectrum of a nascent PE sample at  $101\ ^\circ\text{C}$ . The crystalline resonance appears at  $33.1\ \text{ppm}$ , and the resonance from the amorphous chains is at  $31.2\ \text{ppm}$ . The downfield shift of the amorphous material in the nascent sample relative to the melt-crystallized sample is indicative of a smaller contribution from the gauche conformation in the former. (C) A spectrum of the nascent sample shown in B after raising the temperature to  $128\ ^\circ\text{C}$  and (D) after raising the temperature to  $137\ ^\circ\text{C}$ . The spectra at  $128$  and  $137\ ^\circ\text{C}$  establish that the  $31.2\ \text{ppm}$  resonance is present before melting.

The former is just below the onset of the melting endotherm in the DSC, and the latter is approximately at the middle of the broad ( $130$ – $142\ ^\circ\text{C}$ ) melting endotherm. It is apparent that the broad high-field peak ( $31.2\ \text{ppm}$ ) in the  $137\ ^\circ\text{C}$  spectrum was present at  $128\ ^\circ\text{C}$  and was not created by the melting. The peak due to molten segments is at  $30.6\ \text{ppm}$ . These spectra were taken with a contact time of  $200\ \mu\text{s}$  which serves to strongly attenuate the contribution from the molten phase whose high degree of mobility renders the cross polarization inefficient.<sup>11,13</sup> Otherwise, the spectrum at  $137\ ^\circ\text{C}$  is strongly predominated by this resonance.

**Wide-Line Separation (WISE) Spectra.** Recently, Spiess<sup>21,22</sup> and co-workers demonstrated the application of 2D WISE MAS spectroscopy in the observation of  $^1\text{H}$  line shapes of individual components in heterogeneous samples such as semicrystalline polymers or polymer blends. The pulse sequence consists of a  $^1\text{H}$   $\pi/2$  pulse followed by an incremented proton evolution time ( $t_1$ ), after which the proton magnetization is transferred to  $^{13}\text{C}$  via Hartmann–Hahn cross polarization, i.e.,  $\pi/2$  ( $^1\text{H}$ )– $t_1$ –CP–acquisition. Slices at individual  $^{13}\text{C}$  resonances in a 2D data set reveal the  $^1\text{H}$  line widths of the various domains within a sample. Figure 3 shows two such slices from separate runs showing noncrystalline  $^1\text{H}$  line shapes of nascent PE (bottom) and melt-crystallized PE (top). It is apparent that the line width of the amorphous chains in the former is substantially greater than the corresponding protons of the melt-crystallized material. Molecular motion serves to reduce the  $^1\text{H}$ – $^1\text{H}$  dipolar interaction that determines these  $^1\text{H}$  line widths. In order to affect the line width, a fraction of the motion must reorient the  $^1\text{H}$ – $^1\text{H}$  internuclear vectors on a time scale on the order of the inverse of the dipolar interaction, i.e., *ca.*  $10$ – $20\ \mu\text{s}$ . The reduced mobility in the amorphous phase of nascent PE relative to the melt-crystallized material is reflected in

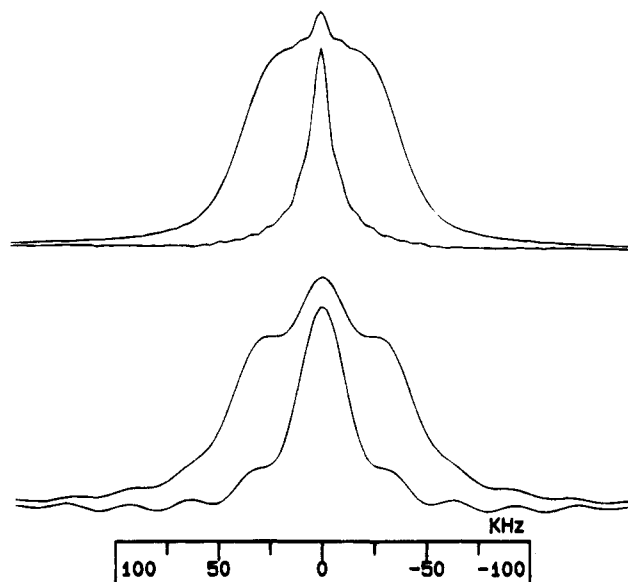


**Figure 3.** Slices from 2D WISE experiments on PE taken at room temperature. (Bottom) The traces reveal the line shape of the protons in the amorphous (narrow) and crystalline domains (broad) of nascent PE. There is some overlap between the  $^{13}\text{C}$  resonances from the crystalline and amorphous phases (cf. Figure 1); thus there is not a clean separation of the crystalline and amorphous line shapes. (Top) The traces show the line shape of the corresponding protons in melt-crystallized PE. The crystalline  $^1\text{H}$  line shape is very similar in both samples, but the amorphous line width is significantly narrower in the melt-crystallized material due to substantially greater molecular mobility. Spectra were obtained at  $75.3\ \text{MHz}$  using a spectral window of  $4\ \text{kHz}$  in the  $f_2$  dimension and  $250\ \text{kHz}$  in the  $f_1$  dimension ( $t_1$  varying from  $0.1$  to  $64\ \mu\text{s}$  for the experiments on nascent PE and from  $0.1$  to  $252\ \mu\text{s}$  for experiments on melt-crystallized PE).

the greater line width. The line shapes of the rigid crystalline protons of the samples are the same, with widths of  $>ca.\ 60\ \text{kHz}$ .

## Discussion

The morphological differences between nascent and melt-crystallized PE are readily observable in  $^{13}\text{C}$  MAS spectra both at room temperature and at temperatures just below the melting point. The latter consists of two resonances at elevated temperatures ( $33.1$  and  $30.6\ \text{ppm}$ ) and the former three ( $33.1$ ,  $31.2$ , and  $30.6\ \text{ppm}$ ).<sup>23</sup> While the resonance from the crystalline peak of the nascent PE is broader than the corresponding resonance in the melt-crystallized sample due to the less perfect nature of the crystals, the more obvious dissimilarities in these spectra arise more from the amorphous phase; the shift to higher field observed in the melt-processed sample relative to the nascent is consistent with an increase in the population of the conformers other than the all-trans conformation.<sup>13</sup> At any and all temperatures, the chemical shift of the amorphous resonance is at higher field in melt-crystallized material than in nascent material. The most likely cause of this is higher mobility and a greater contribution in melt-crystallized PE from the gauche conformer to conformational averaging. The chemical shift of the sharp resonance from molten PE is about  $30.6\ \text{ppm}$  (see Figure 2D). This shift only slowly moves downfield as the temperature is lowered. The more mobile amorphous material generally studied is created in PE only after melt processing. In particular, the evidence from the WISE MAS experiments shows that motion in the amorphous domains is

significantly less than that in material which has been crystallized from the melt, and the irreversible nature of these changes in morphology brought about by melting is clearly demonstrated by the  $^{13}\text{C}$  CPMAS experiments. As outlined above, the molten state of the polymer on the catalyst surface allows for substantial entanglement to occur as the globules of polymer expand and meet each other while still in a molten state. The process of melting allows disentanglement of the chains to occur, removing some of the restrictions to movement that are imposed by the cocrystallization of closely spaced globules during the near-coincident events of polymerization and crystallization.<sup>15,16</sup>

Samples heated to about 190 °C for 15 min to complete the melting process did not show the same spectral features when cooled and reheated throughout the same temperature range as above. (e.g., see Figure 2A). The unique morphological features of nascent PE are permanently lost on melting. Not only does the greater amount of entanglements in nascent PE reduce the mobility of the polymer chains in the noncrystalline domains but also the strain results in its higher melting point as measured by fast DSC (heating rates of 10–20 °C min<sup>-1</sup>).

In nascent (or shear-crystallized) samples strain will only increase the melting point if the crystals are intimately linked as a consequence of the special manner of crystallization outlined above. The connections disappear after a first melting so the  $T_m$  value is lowered in both cases by the first melting. The usual interpretation of this lower  $T_m$  has been the disappearance of strain. However, recent DSC data<sup>24–26</sup> obtained using very slow heating rates (1–2 K/h) have been interpreted otherwise: the melting of the nascent or shear-crystallized samples results in a separation into a phase of very highly strained crystals which melt at a much higher temperature still, plus a semiordered melt phase. The 31.2 ppm peak could also be interpreted as arising from this latter phase possessing less mobility than the amorphous phase of melt-crystallized PE and responsible for the persistence of birefringence in the melt.<sup>20</sup> The melting of the highly strained crystalline phase can only be observed by slow calorimetry.<sup>24–26</sup>

The  $^{13}\text{C}$  spectra of Figure 2 show no changes while the sample is annealed at a given temperature for several hours. A referee has suggested that this 31.2 ppm resonance could be attributed to chain segments near row defects within the crystalline region. The number of such defects would be reduced by this heat treatment, but no changes in the spectra are seen as a function of annealing time. Also, the amount of row defects in these nascent samples cannot be much greater than in melt-crystallized ones as the heat of fusion and degree of crystallinity are about the same for both. The difference in  $T_m$  between nascent (140 °C) and melt-crystallized PE (134 °C) persists even after the long annealing times (40 h) of the slow-temperature ramp DSC studies,<sup>24–26</sup> and this is evidence that the differences observed in the  $^{13}\text{C}$  CPMAS spectra of the two materials do not rest within the crystalline structures.

Essentially identical results were found for numerous (in fact all) other polyethylene samples including those from other sources (the only difference being the slightly different temperatures of the DSC melting endotherms of the samples, which change by a few degrees the temperatures at which three separate resonances are visible in the NMR spectrum). Minor differences were observed in the intensity of the 31.2 ppm peak depend-

ing on how rapidly the sample was heated. Significantly, low molecular weight nascent PE (Union Carbide, MW = 37 000, melt index 37) gave the same CPMAS NMR spectra as Figure 2. We, therefore, conclude that the evidence demonstrates significant differences in the mobility of amorphous chains in nascent versus melt-crystallized PE. The spectra of Figure 2 and 3 clearly show that the amorphous material generally studied in the past<sup>6–8</sup> is created only after melt-processing.

Another possible explanation for the origin of this 31.2 ppm resonance is that it belongs to a pseudohexagonal crystal structure created during the melting process. VanderHart,<sup>27</sup> however, has previously reported the chemical shift of solid  $\text{C}_{19}\text{H}_{40}$ , a hydrocarbon which forms a pseudohexagonal (triclinic) structure. The chemical shift was found<sup>27</sup> to be essentially identical to the shift of hydrocarbons which exist in an orthorhombic unit cell, and therefore, if this third peak were to belong to PE in the pseudohexagonal unit cell, the shift would be close to 33.1 ppm. This is not the case. This, along with the evidence of Figure 2 which clearly shows the existence of the peak before melting begins, makes it unlikely that it is due to material in a pseudohexagonal crystal structure.

Jarrett et al.<sup>14</sup> have measured  $^{13}\text{C}$   $T_1$ s of PE reactor powders and found them to be significantly shorter than melt-crystallized samples of similar crystallite dimensions. They concluded that this is due to the enhanced mobility of surface species which produces shorter  $T_1$ s for nearby crystalline domains due to spin diffusion. The thickness of the lamellae will also be relevant to this issue,<sup>28</sup> but such studies of nascent material are lacking. While we have not measured  $T_1$ s in our samples, the longer  $^{13}\text{C}$   $T_1$  found in melt-crystallized versus nascent PE may instead be due to the formation of more perfect crystals, resulting in a decrease in molecular motion within those domains. Measurement of  $^{13}\text{C}$   $T_1$ s before and after annealing would help to answer this question. In any event, the interpretation of  $^{13}\text{C}$   $T_1$ s is complex due to the effects of  $^{13}\text{C}$ – $^{13}\text{C}$  spin diffusion when the spin–lattice relaxation processes are so long (hundreds to thousands of seconds).

## Conclusions

$^{13}\text{C}$  CPMAS spectra show differences between nascent and melt-crystallized PE which are most distinct at elevated temperatures. At all temperatures studied the amorphous resonance of melt-crystallized PE is upfield of the corresponding resonance in nascent material, indicative of a greater contribution from the gauche conformer to the conformational equilibrium of the former. 2D WISE spectra reveal a significantly wider line width for the amorphous protons of nascent versus melt-crystallized PE, indicating lesser mobility in unprocessed PE.

All nascent samples studied, including those from different sources as well as those of low molecular weight, displayed the same spectral features. It is evident that both  $^2\text{H}$  NMR studies of the deuterated nascent polymer as well as measurement of  $^{13}\text{C}$   $T_1$ s of the nascent polymer are warranted. It is likely that  $^2\text{H}$  line shapes and relaxation behavior will provide significant new insights of a more quantitative nature into the unique characteristics of nascent PE and into the effects of strain in semicrystalline polymers in general. In particular, 2D MAS exchange spectroscopy would reveal whether the rate of diffusion of the polymer

chains between crystalline and amorphous domains is altered by the process of melt crystallization.

## References and Notes

- (1) Spiess, H. W. In *Advances in Polymer Science*; Kausch, H. H., Zachmann, H. G., Ed.; Springer-Verlag: New York, 1985; p 23.
- (2) Hentschel, D.; Sillescu, H.; Spiess, H. W. *Polymer* **1984**, *25*, 1078.
- (3) Hentschel, D.; Rosenke, K.; Sillescu, H.; Spiess, H. W. *Polymer* **1980**, *21*, 757.
- (4) Hentschel, D.; Sillescu, H.; Spiess, H. W. *Macromolecules* **1981**, *14*, 1605.
- (5) Spiess, H. W. *Colloid Polym. Sci.* **1983**, *261*, 193.
- (6) Kitamura, R.; Horii, F.; Murayama, K. *Macromolecules* **1986**, *19*, 636.
- (7) VanderHart, D. L. *J. Magn. Reson.* **1987**, *72*, 13.
- (8) Earl, W. L.; VanderHart, D. L. *Macromolecules* **1979**, *12*, 762.
- (9) Kimura, T.; Neki, K.; Tamura, N.; Horii, F.; Nakagawa, M.; Odani, H. *Polymer* **1992**, *33*, 493.
- (10) Schmidt-Rohr, K.; Spiess, H. W. *Macromolecules* **1991**, *24*, 5288.
- (11) Fyfe, C. A. *Solid State NMR for Chemists*; CFC Press: Guelph, Ontario, Canada, 1984.
- (12) VanderHart, D. L.; Khoury, F. *Polymer* **1984**, *25*, 1589.
- (13) Koenig, J. L. *Spectroscopy of Polymers*; American Chemical Society: Washington, DC, 1992.
- (14) Jarrett, W. L.; Mathias, L. J.; Porter, R. S. *Macromolecules* **1990**, *23*, 5164.
- (15) Chanzy, H. D.; Revol, J. F.; Marchessault, R. H.; Lamandé, A. *Colloid Polym. Sci.* **1973**, *251*, 563.
- (16) Chanzy, H. D.; Bonjour, E.; Marchessault, R. H. *Colloid Polym. Sci.* **1974**, *252*, 8.
- (17) Nedkov, E.; Kreteva, M. *Bulg. J. Phys.* **1982**, *9*, 63.
- (18) The effect on  $T_m$  of cross-linking melt-crystallized polymers has been investigated and reported.<sup>19</sup> The cross-links act as impurities and lower  $T_m$  in cases of lightly-cross-linked chains. However, the more highly cross-linked chains melt at higher temperature as observed by slow calorimetry.
- (19) Smook, J.; Pennings, A. J. *Colloid Polym. Sci.* **1984**, *262*, 712.
- (20) Cohen-Addad, J. P.; Feio, G.; Péguy, A. *Polym. Commun.* **1987**, *28*, 255.
- (21) Schmidt-Rohr, K.; Claus, J.; Spiess, H. W. *Macromolecules* **1992**, *25*, 3273.
- (22) Claus, J.; Schmidt-Rohr, K.; Adam, A.; Boeffel, C.; Spiess, H. W. *Macromolecules* **1992**, *25*, 5208.
- (23) While it is possible that a fourth peak representing interfacial material may be present, simulations with four Lorentzians results in fits that were no better than those achieved by simply assuming some minor Gaussian character for the broader peaks.
- (24) Phuong-Nguyen, H.; Delmas, G. *Macromolecules* **1992**, *30*, 408.
- (25) Phuong-Nguyen, H.; Delmas, G. *Macromolecules* **1992**, *30*, 414.
- (26) Delmas, G. *J. Polym. Sci., Part B: Polym. Phys. Ed.* **1993**, *21*, 2011.
- (27) VanderHart, D. L. *J. Magn. Reson.* **1981**, *44*, 117.
- (28) Axelsson, D. E.; Mandelkern, L.; Popli, R.; Mathieu, P. J. *Polym. Sci., Polym. Phys. Ed.* **1983**, *21*, 2319.

MA946099+